CONDITIONS FOR BROADBAND MMIC VOLTAGE-CONTROLLED OSCILLATORS BASED ON THEORY AND EXPERIMENTS

A. Megej, K. Beilenhoff*, and H. L. Hartnagel

Institut für Hochfrequenztechnik, Technische Universität Darmstadt,
Merckstr. 25, D-64283 Darmstadt, Germany. E-mail: *megej@ieee.org*
*Now with United Monolithic Semiconductors (UMS), 91401 Orsay Cedex, France

***Abstract* — A systematic study of maximally broadband VCO designs is undertaken. The theoretical investigations lead to the practical realization of two fully monolithically integrated VCOs based on reflection-type and feedback design techniques. Employing efficient diode tuning, the practical implementations of PHEMT-MMICs exhibit a variation of output frequency of 30% and 45%, respectively.**

I. INTRODUCTION

WIDE-BAND voltage-controlled oscillators are an essential part in a variety of applications. The increasing use of the monolithically integrated circuits (MMICs) has also created the need of high-performance fully monolithically integrated VCOs.

Two basic topologies can be applied for oscillator design using a transistor as active element: Negative differential resistance technique (reflection-type oscillators) and the feedback arrangement [1], [2]. The reflection-type oscillator circuit topology has often been used for RF–VCO circuit design (e.g. [3]-[5]) whereas the feedback-type oscillators have rarely been considered for microwave applications due to their higher complicity [6], [7].

In this paper, both concepts to design broadband VCOs are systematically compared and the advantages of each particular topology are emphasized. The theoretical considerations are confirmed by two examples of broadband fully monolithically integrated MMIC-VCOs manufactured using a commercially available PHEMT process. The measured frequency tuning ranges are $f_{osc} = 4.8 - 6.5\,\text{GHz}$ and $f_{osc} = 4.6 - 7.3\,\text{GHz}$ for the reflection-type and the feedback VCOs, respectively.

II. THEORETICAL CONSIDERATIONS

A. Reflection-Type Voltage Controlled Oscillator

The reflection type oscillator (also called negative resistance oscillator) contains two parts: the active part with the negative input resistance and the resonator. The entire circuitry has to satisfy the following oscillation condition:

$$\Gamma_{res} \cdot \Gamma_{act} = 1 \tag{1}$$

where Γ_{res} and Γ_{act} are the corresponding reflection coefficients of the resonator and the active circuit, respectively.

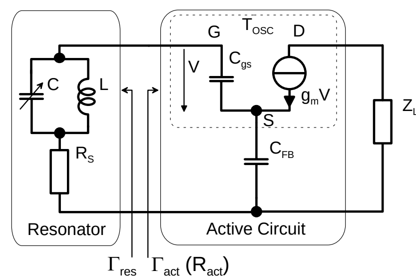

Fig. 1. Basic schematic of the reflection-type VCO with transistor presented by its simplified equivalent circuit (dashed box).

The simplified schematic of the VCO considered is shown in Fig. 1. The active transistor is represented in this figure by a simple model. The resonator circuit is substituted by a capacitor, an inductor, and a resistance. The capacitor C_{FB} realizes the positive feedback in order to achieve the negative differential resistance at the input of the active circuit.

Analyzing this circuit by means of small-signal techniques, the frequency of oscillations and the condition for the transistor's transconductance can be calculated to

$$f_{0,refl} = \frac{1}{2\pi}\sqrt{\frac{1}{L}\cdot\frac{1}{C+\frac{C_{FB}\cdot C_{gs}}{C_{FB}+C_{gs}}}} \tag{2}$$

$$\begin{aligned} g_{m,refl} &= \frac{1}{L}\cdot\frac{C_{FB}\cdot C_{gs}}{C+\frac{C_{FB}\cdot C_{gs}}{C_{FB}+C_{gs}}}\cdot R_s \\ &\sim f\left(R_s\left(V\right), C\left(V\right)\right) \end{aligned} \tag{3}$$

B. Feedback VCO

A feedback oscillator whose simplified schematic is presented in Fig. 2 consists of two sub-circuits: an amplifier and a feedback loop. The two parts have to be designed to fit the following small-signal oscillation condition:

$$S_{21,amp} \cdot S_{21,FB} = 1 \tag{4}$$

where $S_{21,amp}$ and $S_{21,FB}$ are the transmission coefficients of the amplifier and feedback circuits, respectively.

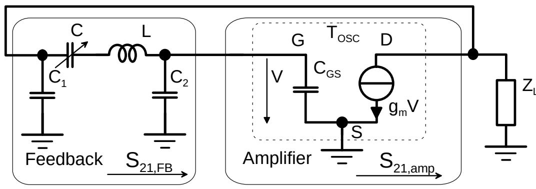

Fig. 2. Basic schematic of the feedback VCO with transistor presented by its simplified equivalent circuit (dashed box).

As in the case of the reflection-type oscillator, the frequency of oscillations and the condition for HEMT's transconductance can be expressed as:

$$f_{0,FB} = \frac{1}{2\pi}\sqrt{\frac{1}{L}\cdot\left[\frac{1}{C}+\frac{1}{C_1}+\frac{1}{C_2+C_{gs}}\right]} \tag{5}$$

$$g_{m,FB} = \frac{C_2+Cgs}{C_1}\cdot\frac{1}{Z_L} = const\cdot\frac{1}{Z_L} \tag{6}$$

C. Comparison of the VCO Design Techniques

Analyzing Eq. (2), it can easily be seen that the reduction of the series connection of C_{gs} and C_{FB} for a given value of C increases the tuneable bandwidth of oscillation.

That means that both C_{gs} and C_{FB} have to be minimized in order to increase the impact of the tuneable capacitance C on the oscillation frequency $f_{0,refl.}$

On the other hand, the analysis of the expression for the resistance of the active circuit

$$R_{act} = -\frac{g_m}{\omega_0^2\cdot C_{gs}\cdot C_{FB}} \tag{7}$$

$$= -g_m\cdot L\cdot\left(\frac{C}{C_{gs}\cdot C_{FB}}+\frac{1}{C_{gs}+C_{FB}}\right) \tag{8}$$

leads to the consequence that both C_{gs} and C_{FB} have to be increased to avoid the strong dependence of the negative differential resistance on the tuning capacitance and, therefore, on the oscillation frequency. Furthermore, since the values of the capacitance C_{gs} and transconductance g_m are determined by the size of the active transistor (actually, the ratio g_m/C_{gs} is almost constant for a given process and a particular bias point), the design latitude is very small. This can also be seen from the Eq. (3) where the transconductance g_m has to be a function of $R_s(V)$ and $C(V)$ in order to fulfill the condition (1). The resistance R_s has a considerable impact on circuit performance although it is a second-order parasitic.

In practice, a compromise has to be found between the transistor size and the value of the feedback capacitance C_{FB} in such a way that the desired value of the negative resistance R_{act} is achieved in a wide frequency band for the smallest transistor T_{osc} and and capacitance C_{FB} possible.

The entire situation concerning the bandwidth of operation and the condition for the transistor's transconductance is more convenient in the case of the feedback oscillator topology. In contrast to the considerations mentioned above and to the equation (3), the expression for the transistor transconductance is constant for given values of C_1 and C_2 and only depends on their ratio (Eq. (6)).

Further, as it can be recognized from the equation (5), the higher the values of the capacitors C_1 and C_2 in comparison to C the more pronounced is the impact of the tuneable capacitance C on the oscillation frequency $f_{0,FB.}$ Moreover, a nice by-effect is achieved: the choice of higher value of C_2 with respect to C_{gs} lowers the impact of technological variations on the oscillation frequency value.

As the result of the above considerations, one may expect higher bandwidth of oscillation and lower output power variation for the VCO's based on the feedback design topology.

III. Circuit Designs Considered and Their Measured Performance

Two voltage-controlled oscillators were designed using the concepts described above. The design basis was the PHEMT process PH25 of UMS. The gate length featured by this process is 0.25 µm. Since varactor diodes are not available with this process, 10×75 µm planar PHEMT diodes with low capacitance-change ratio of $C_{max}/C_{min} \approx 3$ are used for frequency tuning for both oscillator circuits.

In order to make design trade-off between the two oscillator-circuit topologies and define the element values that would result in wide-band oscillators, large-signal S-parameters [9] were used to predict the frequency bandwidth and the output power. This analysis was also performed to demonstrate the difference between both design techniques. During this analysis, the input power was increased till the oscillation conditions (3) and (6) were fulfilled. This procedure was repeated for different values of the tuning voltage $V_{TUNE.}$

A. Negative Resistance Oscillator

The oscillator considered here is similar to the one published in [8]. Moreover, the design was slightly modified in order to increase the bandwidth of operation.

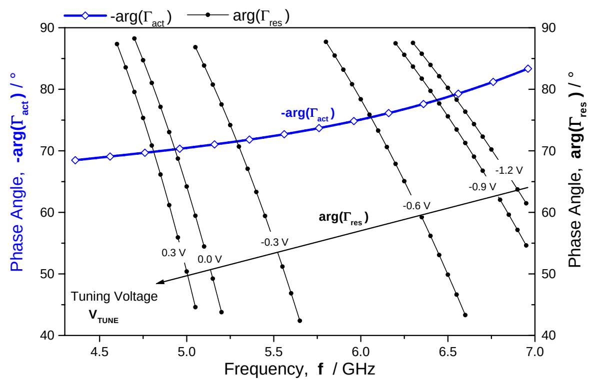

Fig. 3. Reflection-coefficients' phase angle versus frequency of the active circuit and resonator (at different varactor tuning voltages) in the case of the reflection-type VCO.

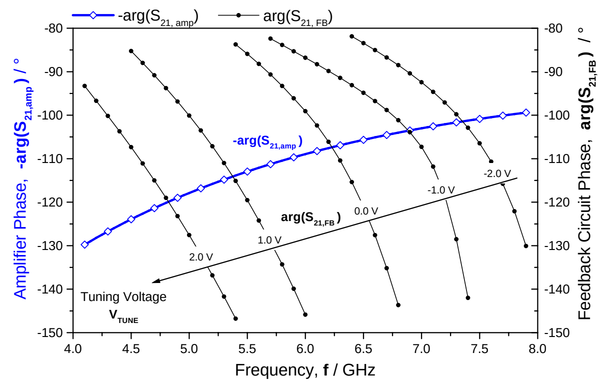

Fig. 4. Phase angle of the transmission coefficients versus frequency of the amplifier and the feedback circuit at different varactor tuning voltages in the case of the feedback VCO.

Analyzing this circuit as described above, a family of curves was generated that is presented in Fig. 3. The phase vs. frequency curves of the resonator reflection coefficient at different diode tuning voltages are shown there as well as the inverted phase of the active circuit. The intersections of these curves give the oscillation frequency at a certain tuning voltage.

From Fig. 3 can be seen that the potential bandwidth of oscillation could be increased by "moving" the curve $-arg\left(\Gamma_{act}\right)$ to lower values (e. g. by decreasing the value of C_{FB} or choosing a smaller active transistor), but the frequency range where condition (3) is fulfilled decreases in this case.

The phase curve of the reflection coefficient Γ_{act} of the active circuit differs from the expected straight line due to the different values of the input power applied to the circuit in order to fulfill condition (3). It had to be altered from $P_{in} = -6.5$ dBm at the lowest frequency up to $P_{in} = 0.8$ dBm to the highest one.

B. Feedback VCO

This circuit represents the further development of the feedback oscillator that was described in detail in [7].

The maximal bandwidth of oscillations would be achieved if all capacitors (C, $C_{1,}$ and C_2) were made variable and the tuning were performed **simultaneously**. However, due to the more difficult DC-voltage supply, only C_1 and C were replaced by the diodes within the first implementation [7]. But in that case, the output power was extremely variable with the tuning voltage. Considering the equation (6), the reason for it can be fixed. Varying the capacitance C_1 while fixing the value of C_2 constant, leads to the fact that the transconductance g_m has to be a function of $C_1 = f\left(V\right)$. Having done so, the same problems that are described above for the case of the reflection-type VCO appeared. As the consequence from this experience, only the capacitor C in Fig. 2 is made variable for this example.

Analyzing separately the amplifier and the feedback circuit using the method described at the beginning of this section, a family of curves were generated that is presented in Fig. 4. This figure shows that the maximal bandwidth of oscillations is obtained. This curve constellation was achieved by optimizing the values of the feedback circuit — that actually is a band-pass filter — as well as by introducing a small series inductance between the passive part and the gate of the active transistor (not shown in Fig. 2).

The increase of the tuning-voltage range with the feedback VCO ($\Delta V_{TUNE} \approx 4$ V in comparison to $\Delta V_{TUNE} \approx 2.5$ V for the reflection-type realization) is a further advantage of this design topology. Due to the fact that there is no RF connection between diodes and ground, positive tuning voltages are possible without significant reduction of the loop gain. This effect also helps to increase the entire bandwidth of VCO operations.

C. Measured Results

On-wafer measurements of the circuits (VCOs including corresponding buffer amplifiers, which cannot described here in detail) were performed employing the spectrum analyzer HP8565E. In Fig. 5, measured curves of the oscillation frequency and the output power of both buffered VCO realizations are shown.

The reflection-type oscillator provides oscillations within the frequency range of $f_{osc,refl} = 4.84{-}6.54$ GHz that corresponds to the relative bandwidth of $\Delta f_{refl}/f_0 = 29.8\,\%$. The oscillation frequency dependence on the tuning voltage exhibits the non-linear behavior typical for this kind of VCOs. The mean output power of this circuit was measured

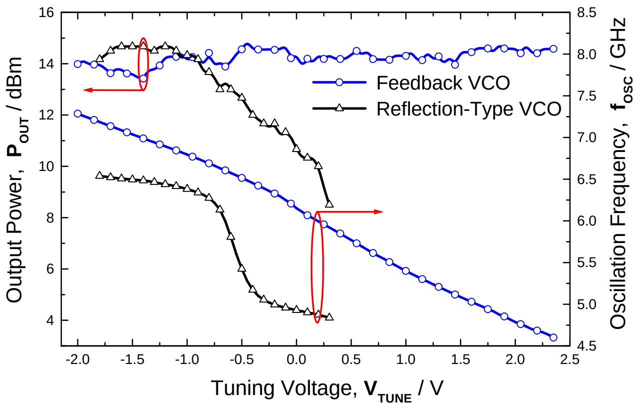

Fig. 5. Measured oscillation frequency and output power of the buffered oscillators designed using different techniques

as $P_{out,refl} = 11.6$ dBm. Confirming the consideration described in Section II *C.*, the variation of this value is rather high and amounts to $\Delta P_{out,refl} = \pm 3.1$ dBm.

The feedback VCO generates RF-power in a wide range of $f_{osc,FB} = 4.60 - 7.28$ GHz that amounts to a very high value of the relative bandwidth of $\Delta f_{FB}/f_0 = 45.1\,\%$. Furthermore, the output power of this circuit exhibits a value of $P_{out,FB} = 14.1$ dBm with a very low variation that was measured to be as high as $\Delta P_{out,FB} = \pm 0.7$ dB. This behavior confirms the theoretical considerations.

IV. Conclusion

In this paper, the detailed analysis was applied to the reflection-type and the feedback VCO design technique with the aim to increase the frequency bandwidth of oscillations. Both circuit topologies were compared to each other in view of broadband circuit design.

In order to prove the considerations made, two practical oscillator realizations were presented and their measured performance was discussed. Incorporating integrated planar PHEMT-diode tuning, the circuits provide frequency tuning in a wide frequency range with 30% and 45% relative bandwidth. Figures 6 and 7 show the microphotographs of the circuits manufactured.

As the result, the superiority of the feedback topology for broadband VCO design could be demonstrated. This includes the larger bandwidth of oscillations, the more linear frequency-voltage characteristic and the flatter power course. Here, design techniques were shown that allow the realization of wide-band microwave oscillators even in the case when varactor diodes with high capacitance-change ratio are not available. The oscillators presented here — in particular the feedback VCO — can find use in applications that require wide frequency tuning ranges, e. g. sensors.

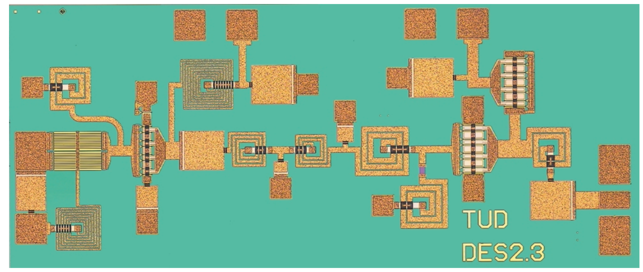

Fig. 6. Microphotograph of the buffered VCO based on the negative resistance technique. Dimensions: $2.4 \times 1.0\,\mathrm{mm}^2$.

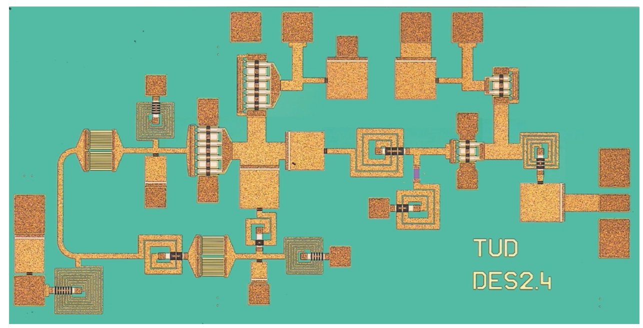

Fig. 7. Microphotograph of the buffered VCO incorporating the feedback topology. Dimensions: $2.4 \times 1.3\,\mathrm{mm}^2$.

Acknowledgment

This work was supported by the Adam Opel AG, Rüsselsheim, Germany. Thanks are also due to the staff of UMS for MMIC manufacturing.

References

[1] G. D. Vendelin, A. M. Pavio, and U. L. Rohde, *Microwave circuit design using linear and nonlinear techniques*, New York: Wiley, 1990.

[2] A. Sweet, *MIC&MMIC amplifier and oscillator circuit design*, Norwood, MA: Artech House, 1990.

[3] B. N. Scott and G. E. Brehm, "Monolithic voltage controlled oscillator for X and Ku-bands," *1982 IEEE MTT-S Int. Microwave Symp. Dig.*, vol. 1, pp. 482–485, June 1982.

[4] J. E. Andrews, T. J. Holden, K. W. Lee, and A. F. Podell, "2.5 – 6.0 GHz broadband GaAs MMIC VCO," *1988 IEEE MTT-S Int. Microwave Symp. Dig.*, vol. I, pp. 491–494, May 1988.

[5] M. Ahdjoudi, A. Boudiaf, and P. Pouvil, "A pseudomorphic HEMT monolithic K-Band VCO," in *26th European Microwave Conf. Proc.*, vol. 1, pp. 101–103, Sept. 1996.

[6] H. J. Siweris, H. Tischer, T. Grave, W. Kellner, "A monolithic W-band HEMT VCO with feedback topology," *1999 IEEE MTT-S Int. Microwave Symp. Dig.*, vol. 1, pp. 17–20, June 1999.

[7] A. Megej, K. Beilenhoff, and H. L. Hartnagel, "Fully monolithically integrated feedback voltage controlled oscillator," *IEEE Microwave Guided Wave Lett.*, vol. 10, pp. 239–241, June 2000.

[8] ——, "Fully integrated PHEMT voltage controlled oscillator with very high tuning bandwidth," in *30th European Microwave Conf. Proc.*, vol. 1, pp. 176–179, Oct. 2000.

[9] *Microwave Design System – User's Guide. Component Catalog, Vol. 2: Control Elements & Sources*, pp. 13-8 – 13-13. Santa Clara: Hewlett-Packard, 1997.